Available online at www.sciencedirect.com
SCIENCE DIRECT
Thermochimica Acta 441 (2006) 127–131
thermochimica acta
www.elsevier.com/locate/tca

The linear thermal expansion and the thermal diffusivity measurements for near-stoichiometric (U, Ce)O_2 solid solutions

Dong-Joo Kim [a,b,*], Yong-Soo Kim [a], Si-Hyung Kim [b], Jong-Heon Kim [b], Jae-Ho Yang [b], Young-Woo Lee [b], Han-Soo Kim [b]

[a] *Department of Nuclear Engineering, Hanyang University, Seoul 133-791, South Korea*
[b] *Korea Atomic Energy Research Institute, P.O. Box 150, Yuseong, Daejeon 305-353, South Korea*

Received 2 September 2005; received in revised form 25 November 2005; accepted 8 December 2005

Abstract

The thermal diffusivities of near-stoichiometric (U, Ce)O_2 solid solutions containing CeO_2 up to 22 mol% were investigated in the temperature range of 298–1273 K using the laser flash method. Also, linear thermal expansion measurements were performed in the temperature range of 298–1673 K using a thermomechanical analysis. The thermal conductivities were determined by a calculation of the thermal diffusivity, the density and the specific heat. The thermal conductivities of the tested samples could be expressed as a function of the temperature by the phonon conduction equation $k = (A + BT)^{-1}$. The thermal conductivity decreased gradually with an increasing Ce content. This was attributable to the increasing lattice defect thermal resistance caused by the U^{4+}, Ce^{4+} and O^{2-} ions as phonon scattering centers.

Keywords: Thermal conductivity; Linear thermal expansion; Uranium–cerium oxide; Laser flash method; Thermomechanical analysis

1. Introduction

In the investigation on nuclear reactor materials, the importance of cerium and cerium oxide is emphasized as one of the major fission products produced in a nuclear fuel under nuclear reactor operation. Further, cerium oxide has often been used as a simulating material for plutonium oxide. Although cerium oxide cannot duplicate the behaviors of plutonium oxide exactly, it has been used owing to its similar tendency of the chemical/thermodynamic behaviors and a convenience in handling [1–3].

In the research of mixed oxide fuel (MOX) using cerium oxide, 20–30 mol% CeO_2 contents are mainly used to simulate a fast breeder reactor (FBR) fuel composition, while (U, Ce)O_2 properties data for a low content (below 20 mol%) are required in the relevant research of a MOX fuel for a pressurized water reactor (PWR) [4].

The thermal conductivity of nuclear fuel materials is the most important property to evaluate the fuel performance in a nuclear reactor, because this property affects the fuel centerline temperature, operating power efficiency, safety, release of the fission product, etc. The thermal conductivity of oxide fuel materials decreases with the fission product forming a solid solution, the perturbation of the stoichiometry for the fuel element, increasing burnup, etc. In this regard, the thermal conductivities of UO_2 and various doped-UO_2 have been intensively studied by many investigators [5–15].

In the present work, the thermal diffusivities of near-stoichiometric (U, Ce)O_2 solid solutions containing CeO_2 up to 22 mol% were measured in the temperature range of 298–1273 K using the laser flash method. Also, the linear thermal expansion measurements for the samples were performed in the temperature range of 298–1673 K. The coefficient of the linear thermal expansion (CTE) and the density were calculated from the measured thermal expansion data. The thermal conductivities were determined by a calculation of the density, the thermal diffusivity and the specific heat.

* Corresponding author. Tel.: +82 42 868 8867; fax: +82 42 868 8868.
E-mail address: djkim@kaeri.re.kr (D.-J. Kim).

0040-6031/$ – see front matter © 2005 Elsevier B.V. All rights reserved.
doi:10.1016/j.tca.2005.12.009

2. Experimental

Various contents of CeO_2 (Aldrich, 99.9%) powders were added to Integrated Dry-Route UO_2 (IDR-UO_2), supplied by British Nuclear Fuel plc. (BNFL), and mixed using a Turbula^{TM} mixer for 1 h. The powder mixtures were milled using an attrition mill for 4 h. Green pellets for the milled powder mixture were formed by a pressing at about 300 MPa using a small amount of lubricant (Zn stearate). The pellets were sintered at 2023 K for 4 h in a flowing H_2 atmosphere [15]. The sizes of the sintered pellets were about 8.5 mm in diameter and 12–13 mm in height.

For the purpose of an observation on the formation of the solid solution, and a calculation of the theoretical densities, the X-ray diffraction peak of a sample was measured by X-ray diffractometry (XRD, Mac Science, MAC-M03XHF) from $2\theta = 10^\circ$ to 120° at room temperature using a Cu Kα target. The step scanning method was used (counting time = 5 s, step width = 0.05°).

In the temperature range of 298–1673 K, the axial directional length changes of the pellets – initial length was about 12–13 mm – were measured under a flowing argon atmosphere using a Thermo-Mechanical Analyzer (TMA, SETARAM, TMA92), and a heating rate of 5 K/min, according to the ASTM designation [16]. The density was calculated using the measured thermal expansion data.

Samples for the thermal diffusivity measurement were cut to 0.9–1.1 mm in thickness and 6 mm in diameter from a sintered pellet and polished. In the temperature range of 298–1273 K, the thermal diffusivity was measured using a Laser Flash Apparatus (Netzsch, LFA-427). The measurements of the thermal diffusivity were carried out three times at every test temperature step in a vacuum (10^{-4} Pa to 10^{-5} Pa). The thermal conductivities were calculated from the density, the thermal diffusivity and the specific heat which was calculated by the Neumann–Kopp's law using the literature data on UO_2 and CeO_2 [17–22].

3. Results and discussion

It was observed that CeO_2 in the UO_2 matrix was fully formed as a solid solution in this composition range using the X-ray diffraction. The lattice parameters were obtained using the measured peak data [23]. Fig. 1 shows that the lattice parameter linearly decreased with an increasing Ce content. Based on the fact that the data points are on a straight line, i.e. the measured data follow the Vegard's law, it can be considered that the oxygen-to-metal (O/M) ratio for these samples is the stoichiometric or the near-stoichiometric state.

Even if oxygen vacancies were formed at a high temperature, an oxygen pick-up during storage in air could fill the oxygen vacancies since the solid solution containing an oxygen deficiency is very susceptive to oxidation [24]. That is to say, although the samples were sintered in a H_2 atmosphere, the O/M ratio changed to be the near-stoichiometric state (2.00–1.99).

By many investigators [10,13,25–28], hypo-stoichiometric (U, Ln)O_{2-x} has been reported to oxidize easily in air, even at room temperature, to almost a stoichiometric composition.

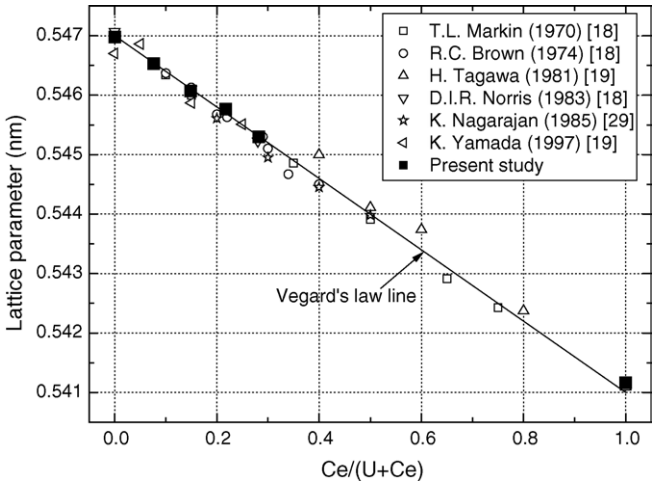

Fig. 1. The measured lattice parameters and literature data of (U, Ce)O_2 as a function of the Ce contents.

So, although the O/M ratio of the samples was not measured in this study, it can be considered that the deviation from stoichiometric in this sample composition range is assumed to be negligible.

3.1. Linear thermal expansion measurements

For the sample of $(U_{1-y}Ce_y)O_2$ ($0 \le y \le 0.22$), the length changes of the sintered pellet were measured using TMA from room temperature to 1673 K in a flowing argon atmosphere. The linear thermal expansions of a sample forming a solid solution increased with an increasing Ce content (Fig. 2). This trend can be correlated with the higher density and melting point of UO_2 (10.96 g/cm^3, 3100 K) as compared to that of CeO_2 (7.65 g/cm^3, 2673 K). The measured linear thermal expansion was fitted as a function of the temperature using a cubic polynomial regression ($\Delta L/L\,(\%) = a + bT + cT^2 + dT^3$), with the fitting parameters given in Table 1, where T is an absolute temperature (K) and T_o is 298 K.

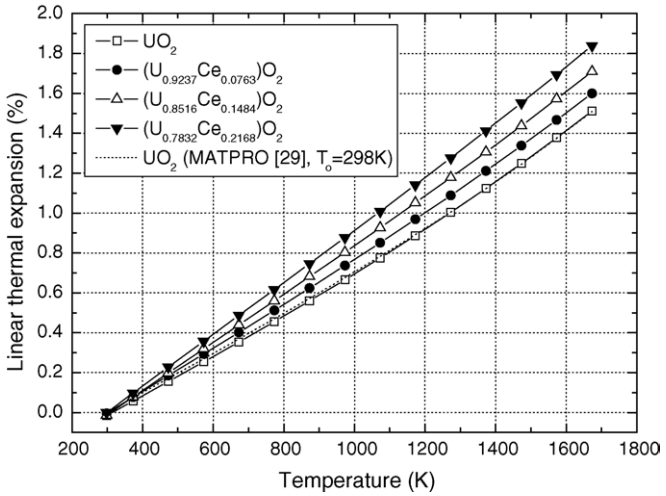

Fig. 2. Measured linear thermal expansion using the TMA method for (U, Ce)O_2 as a function of the Ce content.

Table 1
The fitting parameters of the linear thermal expansion (%) for all the samples as a function of the temperature ($100 \cdot \Delta L/L_o = a + bT + cT^2 + dT^3$), 293–1673 K

Composition	a	b ($\times 10^{-3}$)	c ($\times 10^{-7}$)	d ($\times 10^{-11}$)
UO_2	−0.28706	0.92445	0.08642	4.84138
$(U_{0.924}Ce_{0.076})O_2$	−0.32599	1.09000	−0.46248	4.94623
$(U_{0.852}Ce_{0.148})O_2$	−0.38030	1.30000	−1.65460	8.05768
$(U_{0.783}Ce_{0.217})O_2$	−0.39764	1.36000	−1.04597	5.43329

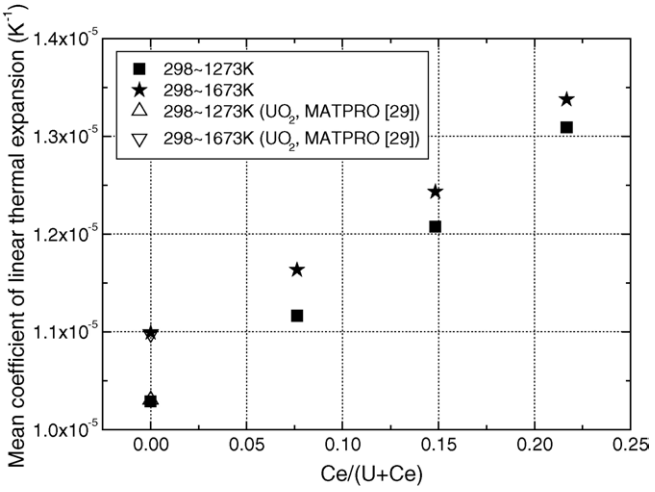

Fig. 3. Mean coefficient of the linear thermal expansion of (U, Ce)O_2 as a function of the Ce content at 1273 K and 1673 K. These results were in good agreement with the reference data.

The mean coefficients of the linear thermal expansion were calculated using the following equation [29]:

$$\alpha_p(l) = \frac{1}{L_{298}}\left(\frac{dL}{dT}\right)_p \quad (1)$$

Fig. 3 shows the calculated results from room temperature to 1273 K and 1673 K, respectively. It shows that the coefficient gradually increases with an increasing Ce content.

Finally, from the data of the measured length changes and the following relationship [29], the density change by thermal expansion was fitted using a cubic polynomial regression as a function of the temperature:

$$\frac{\Delta\rho}{\rho_o} = \frac{1-(1+\Delta L/L_o)^3}{(1+\Delta L/L_o)^3} \quad (2)$$

The fitted parameters are shown in Table 2. For the comparison of the different compositions, it was expressed as the relative density, where the density at room temperature was normalized to 1 (Fig. 4).

Table 2
The fitting parameters of the density for all the samples as a function of the temperature (ρ (g/cm^3) $= a + bT + cT^2 + dT^3$), 293–1673 K

Composition	a	b ($\times 10^{-4}$)	c ($\times 10^{-8}$)	d ($\times 10^{-11}$)
UO_2	11.04447	−3.05135	−0.08626	−1.34855
$(U_{0.924}Ce_{0.076})O_2$	10.78779	−3.51866	1.89979	−1.41041
$(U_{0.852}Ce_{0.148})O_2$	10.53816	−4.09061	5.67156	−2.34803
$(U_{0.783}Ce_{0.217})O_2$	10.28983	−4.19046	3.93252	−1.53539

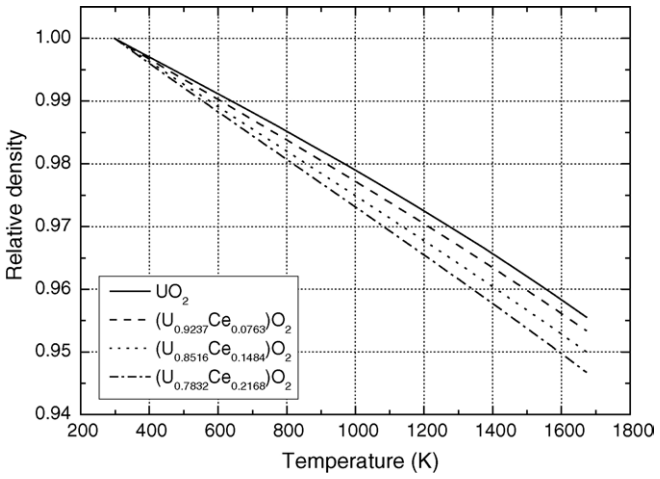

Fig. 4. Relative density variation with the temperature of (U, Ce)O_2 as a function of the Ce content.

3.2. Thermal conductivity calculations with the thermal diffusivity, density and specific heat

The thermal conductivity was calculated using the equation of $k = \alpha_M c_p \rho_M$. The thermal diffusivity, α_M, was measured using the laser flash method (Fig. 5). The density, ρ_M, was calculated from the measured expansion data (Fig. 4 and Table 2). The specific heat, c_p, was calculated from the literature data for individual component materials using Neumann–Kopp's law. For the comparison of the different compositions, all the thermal conductivities were normalized to a 95% theoretical density using the modified Loeb equation [30] and the following expression:

$$k_M = k_{th}(1 - P\eta), \quad (3)$$

where k_{th} is the thermal conductivity of a fully dense material, k_M the thermal conductivity of a sample with a density of ρ_M, P the porosity, η the experimental parameter expressed as $2.6 - 5 \times 10^{-4}T$ [29] and T is the temperature for the measurements (K).

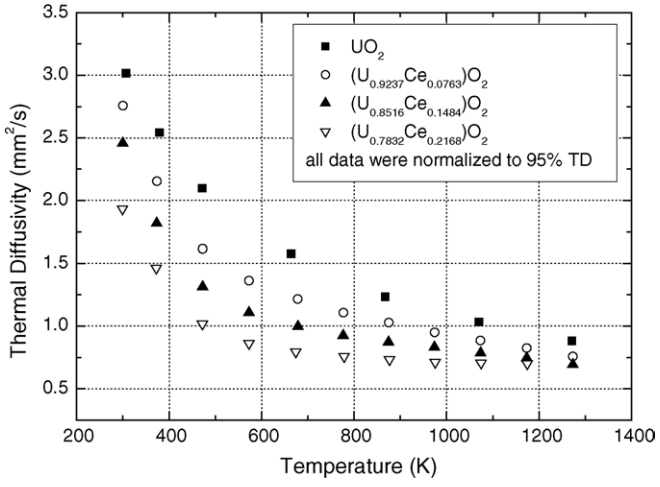

Fig. 5. Thermal diffusivities of (U, Ce)O_2 with varied Ce contents as a function of the temperature.

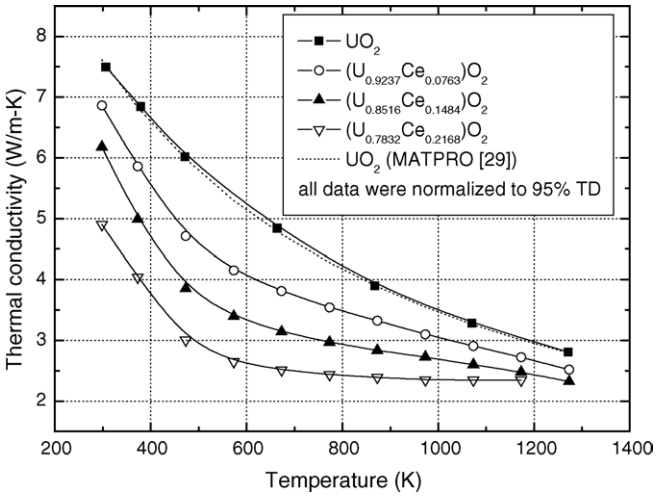

Fig. 6. Thermal conductivities of (U, Ce)O_2 with varied Ce contents as a function of the temperature.

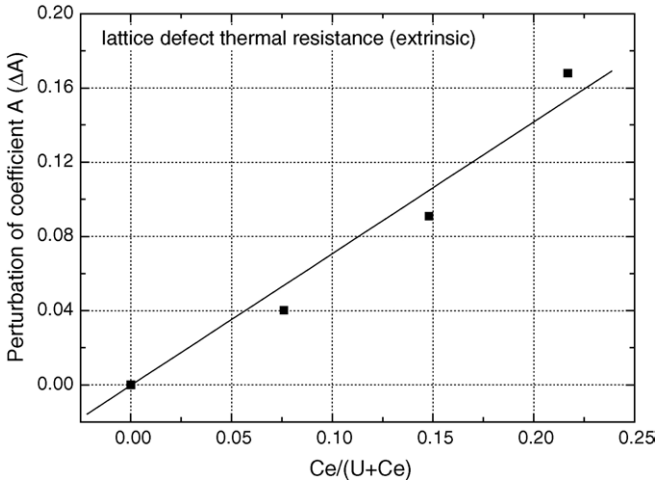

Fig. 7. Relationship between the perturbation of the fitted coefficient *A* (lattice defect thermal resistance) and the Ce content in the (U, Ce)O_2.

Fig. 6 shows the gradually decreasing thermal conductivities with an increasing Ce content. The thermal conductivity data were fitted using the phonon conduction equation $k = (A + BT)^{-1}$, because it is sufficient enough to describe the thermal conductivity using the lattice contribution only, in the temperature region of this experiment (from room temperature to 1273 K). The fitted values of coefficients *A* and *B* for each sample are shown in Table 3.

The following equation for the thermal resistance – inverse of the phonon conduction equation – indicates the relationship between *A* and *B*, the parameters of the lattice contribution to the thermal conductivity:

$$w = \frac{1}{k} = w_l + w_p = A + BT, \quad (4)$$

$$A = A_o + \Delta A, \qquad B = B_o + \Delta B, \quad (5)$$

where w is the thermal resistance, w_l the lattice defect thermal resistance (A), w_p the intrinsic thermal resistance (BT), A_o and B_o the coefficients for UO_2 and ΔA and ΔB are the perturbations of the coefficient.

In Fig. 7, it is shown that the lattice defect thermal resistance increases with an increasing Ce content. Because the O/M ratio of the samples is the near-stoichiometric state, it can be thought that the Ce content is primarily responsible for the thermal conductivity of (U, Ce)O_2. This is mainly attributable to the increasing lattice defect thermal resistance caused by the U^{4+}, Ce^{4+} and O^{2-} ions as point defects, i.e. phonon scattering centers. The mean free path of the phonon can be decreased in the presence of point defects in the solid. Also, the mass difference between the host (U) and the substituted atom (Ce) can be thought to be point defects which interrupt a transport of the heat energy.

Table 3
Calculated values of *A* and *B* of $(U_{1-y}Ce_y)O_2$ from the fitting relationship

Composition	*A* (m K/W)	*B* (m/W)
UO_2	0.06019	0.00023
$(U_{0.924}Ce_{0.076})O_2$	0.10037	0.00023
$(U_{0.852}Ce_{0.148})O_2$	0.15111	0.00022
$(U_{0.783}Ce_{0.217})O_2$	0.22812	0.00020

Fig. 8 shows that the intrinsic thermal resistance decreases with an increasing Ce content; however, the perturbation of the coefficient *B* is very small. The phonon–phonon scattering (the intrinsic thermal resistance) is due to the anharmonic components of the crystal vibrations, i.e. lattice anharmonicity increases with the mass difference between the anions and cations in the ionic material [31]. But, in these samples, the mass difference between the host (U^{4+}) and the substituted cation (Ce^{4+}) is very large, so the influence of Ce^{4+} can be thought to be relatively small.

In conclusion, the following recommended equation for the relationship between the thermal conductivity and the Ce content (y, mole fraction) in near-stoichiometric (U, Ce)O_2 solid solution was obtained using the fitted results:

$$k = \frac{1}{(0.06019 + 0.70988y) + (0.00023 - 1.07768 \times 10^{-4}y)T} \quad (0 \le y \le 0.22) \quad (6)$$

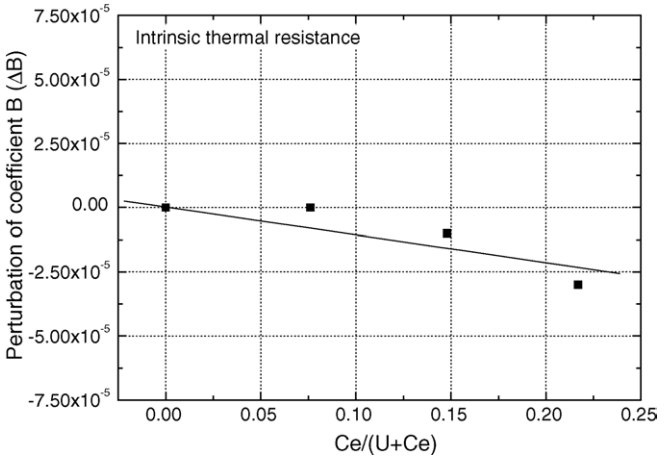

Fig. 8. Relationship between the perturbation of the fitted coefficient *B* (intrinsic thermal resistance) and the Ce content in the (U, Ce)O_2.

4. Conclusions

The thermal diffusivities of near-stoichiometric (U, Ce)O_2 solid solutions containing CeO_2 up to 22 mol% were measured in the temperature range of 298–1273 K using the laser flash method. Also, linear thermal expansion measurements for the samples were performed in the temperature range of 298–1673 K.

1. The linear thermal expansions of a sample forming a solid solution increased with an increasing Ce content. This trend can be correlated with the higher density and melting point of UO_2 (10.96 g/cm^3, 3100 K) as compared to that of CeO_2 (7.65 g/cm^3, 2673 K).
2. The thermal conductivities of (U, Ce)O_2 gradually decreased with an increasing Ce content. It was mainly attributable to the increasing lattice defect thermal resistance caused by the U^{4+}, Ce^{4+} and O^{2-} ions as point defects, i.e. phonon scattering centers. But the intrinsic thermal resistance is hardly affected with an increasing Ce content.

Acknowledgement

The authors acknowledge that this work has been performed under the Nuclear Mid- and Long-term R&D Projects supported by the Ministry of Science and Technology in Korea.

References

[1] D.I.R. Norris, P. Kay, J. Nucl. Mater. 116 (1983) 184.
[2] K. Yamada, S. Yamanaka, T. Nakagawa, M. Uno, M. Katsura, J. Nucl. Mater. 247 (1997) 289.
[3] K. Nagarajan, R. Saha, R.B. Yadav, S. Rajagopalan, K.V.G. Kutty, M. Saibaba, P.R. Vasudeva Rao, C.K. Mathews, J. Nucl. Mater. 130 (1985) 242.
[4] B.H. Lee, Y.H. Koo, J.S. Cheon, J.Y. Oh, H.K. Joo, D.S. Sohn, J. Korean Nucl. Soc. 34 (5) (2002) 482.
[5] D.G. Martin, J. Nucl. Mater. 110 (1982) 78.
[6] M. Hirai, S. Ishimoto, J. Nucl. Sci. Technol. 28 (11) (1991) 995.
[7] M.V. Krishnaiah, G. Seenivasan, P. Murti, C.K. Mathews, J. Nucl. Mater. 306 (2002) 10.
[8] R. Gibby, BNWL-927, Pacific Northwest Lab., Battelle Northwest, Richland, WA, 1969.
[9] R. Gibby, J. Nucl. Mater. 38 (1971) 163.
[10] S. Fukushima, T. Ohmichi, A. Maeda, H. Watanabe, J. Nucl. Mater. 102 (1981) 30.
[11] S. Fukushima, T. Ohmichi, A. Maeda, H. Watanabe, J. Nucl. Mater. 105 (1982) 201.
[12] G.J. Hyland, J. Nucl. Mater. 113 (1983) 125.
[13] S. Fukushima, T. Ohmichi, A. Maeda, M. Handa, J. Nucl. Mater. 114 (1983) 312.
[14] H.J. Lee, C.W. Kim, J. Korean Nucl. Soc. 8 (2) (1976) 81.
[15] D.J. Kim, S.H. Na, Y.K. Kim, Y.W. Lee, Y.S. Kim, J. Korean Ceram. Soc. 41 (8) (2004) 588.
[16] ASTM Designation, E831-03.
[17] Outokumpu HSC Chemistry 4.0 for Windows, Chemical Reaction and Equilibrium Software with Extensive Thermochemical Database, 1999.
[18] E.H.P. Cordfunke, R.J.M. Konings, Thermochemical Data for Reactor Materials and Fission Products, Amsterdam, North Holland, 1990.
[19] D.T. Hagrman, NUREG/CR-6150, EGG-2720, Vol. IV, U.S. Nuclear Regulatory Commission, 1993.
[20] J.K. Fink, J. Nucl. Mater. 279 (2000) 1.
[21] J.J. Carbajo, G.L. Yoder, S.G. Popov, V.K. Ivanov, J. Nucl. Mater. 299 (2001) 181.
[22] Y. Arita, T. Matsui, S. Hamada, Thermochim. Acta 253 (1995) 1.
[23] D.J. Kim, Y.W. Lee, Y.S. Kim, J. Nucl. Mater. 342 (2005) 192.
[24] T. Ohmichi, S. Fukushima, A. Maeda, H. Watanabe, J. Nucl. Mater. 102 (1981) 40.
[25] R.J. Beals, J.H. Handwerk, J. Am. Ceram. Soc. 48 (5) (1965) 271.
[26] J.F. Wadier, CEA-R-4507, Fontenay, 1973.
[27] K. Une, M. Oguma, J. Nucl. Mater. 110 (1982) 215.
[28] H. Tagawa, T. Fujino, J. At. Energy Soc. Jpn. 22 (1980) 871.
[29] Material Properties Database, International Nuclear Safety Center, 1999, http://www.insc.anl.gov/matprop/.
[30] A.L. Loeb, J. Am. Ceram. Soc. 37 (1954) 96.
[31] D.R. Olander, Fundamental Aspects of Nuclear Reactor Fuel Elements, TID-26711-P1, 1976, p. 122.